Applied Catalysis B: Environmental 111–112 (2012) 349–359

Contents lists available at SciVerse ScienceDirect

Applied Catalysis B: Environmental

journal homepage: www.elsevier.com/locate/apcatb

Oxy-chlorination as an effective treatment of aged Pd/CeO_2-Al_2O_3 catalysts for Pd redispersion

Panagiota S. Lambrou, Kyriaki Polychronopoulou, Klito C. Petallidou, Angelos M. Efstathiou*

Chemistry Department, Heterogeneous Catalysis Laboratory, University of Cyprus, University Campus, P.O. Box 20537, CY 1678 Nicosia, Cyprus

ARTICLE INFO

Article history:
Received 12 July 2011
Received in revised form 8 October 2011
Accepted 11 October 2011
Available online 17 October 2011

Keywords:
Pd redispersion
X-ray photoelectron spectroscopy
Oxygen storage capacity
Oxy-chlorination treatment
CO oxidation
NO chemisorption

ABSTRACT

The present work reports on the effects of oxy-chlorine gas treatment (use of Cl_2/O_2/He gas mixture) applied on a 5 wt% Pd/20 wt% CeO_2-Al_2O_3 catalyst towards Pd redispersion. X-ray diffraction (XRD), X-ray photoelectron spectroscopy (XPS), high resolution transmission electron microscopy (HR-TEM), temperature programmed reduction in H_2 (H_2-TPR) and *in situ* diffuse reflectance infrared Fourier transformed spectroscopy (DRIFTS) NO chemisorption techniques were employed before and after use of the oxy-chlorine gas treatment to critically evaluate its efficiency. The composition (*x* vol% Cl_2/18 vol% O_2/He), temperature, and time on stream were investigated. The first two parameters were found to largely dictate optimum Pd redispersion, namely the use of a 2 vol% Cl_2/18 vol% O_2/He gas mixture at 500 °C for 1 h, where a significant reduction of an initial Pd mean particle size of 17.3–7.5 nm was obtained. XPS studies revealed that after oxy-chlorine gas treatment followed by H_2 reduction at 500 °C, complete elimination of Cl from the Pd surface was achieved. The oxygen storage capacity (OSC) of the catalyst measured following different oxy-chlorine gas treatments was found to significantly increase. Catalytic activity towards CO oxidation along with *in situ* DRIFTS NO chemisorption studies proved the large effect of the oxy-chlorine gas treatment on increasing the CO oxidation rate and the extent of NO chemisorption. Alternative treatment in oxygen gas atmosphere at high temperatures (500–850 °C) followed by H_2 reduction (300–500 °C) applied over the same catalyst failed to cause significant redispersion of Pd as observed with the oxy-chlorine gas treatment.

1. Introduction

The superiority of Pd towards the catalytic combustion of methane (natural gas) to drive a gas turbine for power generation with low emissions of CO, unburned CH_4, and NO_x of less than 10 ppm has attracted increasing attention in recent years [1–9]. At the same time, Pd is also a very active catalyst for the combustion of lean CH_4 gas mixture at low-temperatures to abate the emissions of methane from the same process. Alumina-supported Pd catalysts promoted by CeO_2 or CeO_2-ZrO_2 solid solutions display excellent activity towards methane combustion [2–4,6–8].

In an effort to develop alternative to Ni-based industrial catalysts for steam reforming of methane, where these catalysts are prone to a large coke formation, noble metal-based catalysts of low loading and particularly Pd (low cost) were investigated (*x* wt% CeO_2-Al_2O_3 was used as a support of Pd) [10,11]. Pd/CeO_2-Al_2O_3 catalytic systems were also explored towards several other important reactions, namely: steam reforming of hydrocarbons [10–13], water-gas shift reaction [14], methanol decomposition [15], hydrodesulfurization (HDS) [16], and "three-way" Pd-only catalysts for gasoline-driven cars emission abatement [17,18]. In the above-mentioned catalytic applications regarding the Pd/CeO_2-Al_2O_3 solids, high temperatures are used which usually result in Pd metal agglomeration and a subsequent significant loss of catalytic activity. Redispersion of supported noble metal catalysts (usually of high cost) into smaller particles for catalytic activity recovery remains a highly desirable objective, when possible. In fact, redispersion of Pt-based catalyst used in petroleum industry has been reported [19,20].

The transformation chemistry of PdO ↔ Pd on supported-Pd catalysts under oxygen and hydrogen gas atmospheres used in high-temperature methane combustion was investigated in an effort to understand persistent hysteresis in reaction rates [21–24]. It was found that Pd particle size and morphology strongly depend on the temperature, partial pressure of O_2 and H_2 treatment and time of exposure (kinetic effect), and the surface tension between Pd (PdO) with the support surface.

The use of chlorine-containing reagents for the redispersion of noble metals in aged industrial catalysts has been reported [25–27]. The intermediate species of the general formula MO_xCl_y is believed

* Corresponding author. Tel.: +357 22 892776; fax: +357 22 892801.
E-mail address: efstath@ucy.ac.cy (A.M. Efstathiou).

0926-3373/$ – see front matter © 2011 Elsevier B.V. All rights reserved.
doi:10.1016/j.apcatb.2011.10.018

to lead to the formation of smaller metal particles at the expense of larger ones. Oxy-chlorination has been used successfully for the regeneration of Pt/Al_2O_3-based industrial reforming catalysts [28,29]. D'Aniello et al. [25] reported that a high degree of reactivation was achieved in the case of monometallic Pt catalysts using a simulating car exhaust gas. Birgersson et al. [30] reported on the feasibility of the oxy-chlorination method in terms of Pd redispersion in a "three-way" catalyst (TWC) that led to high activity regarding CO and HC oxidation, and NO_x reduction. Anderson et al. [31] reported on the redispersion of aged $Pt\text{-}Rh/Ce_xZr_{1-x}O_2$ model TWCs. Improvements in the oxygen storage capacity (OSC) were found to depend on the metal loading.

In the present work, for the first time an in-depth investigation of the effects of oxy-chlorine gas treatment applied over a 5 wt% Pd/20 wt% CeO_2-Al_2O_3 catalyst on Pd metal redispersion, OSC, and the interaction between the metal and the oxygen storage component are investigated. The catalysts were characterized before and after oxy-chlorine gas treatments by several techniques: X-ray diffraction (XRD), X-ray photoelectron spectroscopy (XPS), high resolution transmission electron microscopy (HR-TEM), hydrogen temperature-programmed reduction (H_2-TPR), and OSC measurements. In order to probe redispersion of Pd phase (increase of Pd surface sites per gram of catalyst), the rate of CO oxidation (catalytic activity) and the extent of NO chemisorption (*in situ* DRIFTS studies) were used. Redispersion of PdO phase by oxygen treatments in the 500–850 °C range followed by hydrogen reduction at 500 °C (same temperature used after oxy-chlorine gas treatment) has been also performed for comparison purposes.

2. Experimental

2.1. Preparation of 5 wt% Pd/CeO_2-Al_2O_3 catalyst

In order to create a relatively large mean Pd particle size with a good number density (number of Pd particles per gram of catalyst) population needed for the various characterization and catalytic studies, a 5 wt% Pd metal loading was deposited onto a γ-Al_2O_3 (Aldrich, standard grade)–20 wt% CeO_2 support during a wet impregnation procedure (distilled deionized water, 50 °C). An appropriate amount of $Pd(NO_3)_2$ (Aldrich, 99.999%) was used as a metal precursor. The support material was prepared by impregnating γ-Al_2O_3 (in powder form) with an appropriate amount of $Ce(NO_3)_3{\cdot}6H_2O$ (Aldrich, 99.999%) in distilled de-ionized water at 50 °C, so as to yield a support material with 80 wt% γ-Al_2O_3–20 wt% CeO_2 composition. After drying at 120 °C for 12 h, the support material was calcined in air in the 200–800 °C range with a 1-h stay every 100 °C before impregnation with the palladium precursor compound. After this step, the 5 wt% Pd/20 wt% CeO_2-Al_2O_3 catalyst was dried at 120 °C for 12 h and then stored without further treatment.

2.2. Catalysts characterization

2.2.1. Powder X-ray diffraction studies

The crystal structure of the 5 wt% Pd/γ-Al_2O_3-CeO_2 catalysts before and after any applied oxy-chlorine gas treatment (use of Cl_2/O_2/He gas mixtures) was checked by powder X-ray diffraction (Shimadzu 600 Series Diffractometer with temperature controllable cell (heating attachment HA-1001) able to reach 900 °C) after employing CuKα radiation (λ = 1.5418 Å). The Scherrer equation was used for estimating the volume mean Pd metal particle size. *In situ* XRD studies were conducted under 20% O_2/Ar and 5% H_2/Ar gas flow in the temperature range of 500–850 °C in order to investigate redispersion of Pd under these gas treatments (reference study), and compare their results with those obtained under the oxy-chlorine gas treatments.

2.2.2. X-ray photoelectron spectroscopy (XPS) studies

XPS studies were conducted on a VG Escalab 200 R spectrometer equipped with a hemispherical electron analyzer (SPECS LH-10) and an MgKα (1253.6 eV) X-ray source. The XP spectrometer was maintained at a base pressure of $\sim 8 \times 10^{-10}$ mbar, and it was equipped with a chamber for sample treatment under controlled gas atmosphere (1 atm) and at temperatures lower than 700 °C. A certain region of the XP spectrum was scanned a number of times in order to obtain a good signal-to-noise ratio. The binding energies (BE) were referenced to the spurious C 1s peak (285 eV) used as an internal standard to take into account charging effects. The areas of the peaks were computed by fitting the experimental spectra to Gaussian/Lorentzian curves after removing the background using the Shirley function. Surface atom ratios were calculated from normalised peak area ratios by using the corresponding atomic sensitivity factors. The experimental error in estimating the surface composition and atom ratios is considered to be less than 10%.

2.2.3. H_2-TPR studies

H_2-TPR traces were obtained using 0.1 g of the sample placed in a quartz micro-reactor, the exit of which was connected to a mass spectrometer (Balzer Prisma QMS 200) for *on line* gas analysis [32]. The gas flow rate was 100 NmL/min (5 vol% H_2/Ar) and the heating rate was 30 °C/min (25–850 °C). The H_2 signal ($m/z = 2$) in the mass spectrometer was continuously monitored in order to estimate the rate of reduction of the supported-Pd catalyst investigated. Gas lines from the reactor to the inlet of the mass spectrometer were heated to 120 °C in order to avoid water condensation. The H_2-TPR traces obtained were expressed as reduction rate (μmol H_2/g s) versus temperature, after calibrating the MS signal with a standard H_2 in He diluent gas (1 vol% H_2/He) and using the appropriate material balance.

2.2.4. Oxygen storage capacity (OSC) measurements

The OSC of the 5 wt% Pd/γ-Al_2O_3-20 wt% CeO_2 catalysts before and after the applied oxy-chlorine gas treatments was measured based on the pulse injection method proposed by Yao and Yu Yao [33]. The transient flow-system, the micro-reactor, and the mass spectrometer used have been previously described [32]. The reactive oxygen species present in the catalyst sample is defined as the amount of O_2 consumed during the re-oxidation stage of the H_2/O_2 pulse experiment [33,34]. The latter amount of oxygen (μmol O/g_{cat}) is referred as the "oxygen storage capacity complete", OSCC. The amount of the most reactive (labile) oxygen of the catalyst is defined as the amount of oxygen that reacts during the first oxygen pulse during the re-oxidation stage of the H_2/O_2 pulse experiment, and it is called "oxygen storage capacity", OSC. The amount of catalyst sample used for the OSC/OSCC measurements was 50 mg in powder form diluted with 100 mg of SiO_2. The general experimental procedure applied for OSC measurements was as follows. Initially, the catalyst sample was pretreated in 20% O_2/He gas mixture at a given calcination temperature (T_{calc}) for 1 h. The reactor was then flushed with He for 5 min and then cooled in He flow to the temperature of OSC measurement (T_{OSC}). The catalyst sample was then reacted with one H_2 pulse (50 μmol) at T_{OSC}, flushed with He for 5 min, and then re-oxidized with several successive pulses of O_2 (one oxygen pulse equals 10 μmol) at the same temperature. In the case of OSCC, the sample was reacted with several successive pulses of H_2 at T_{OSC}, flushed with He for 5 min, and then re-oxidized with several successive pulses of O_2 at the same temperature. Reproducibility of all oxygen storage capacity experiments was within 5%.

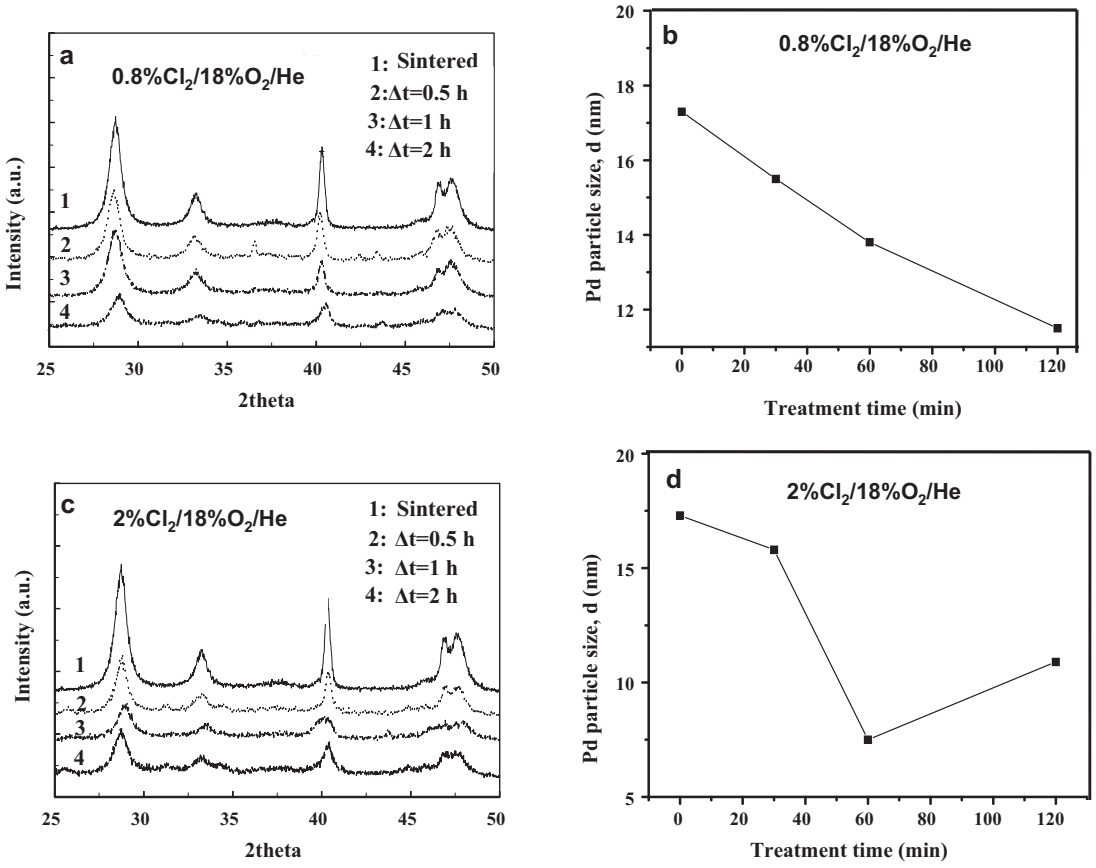

Fig. 1. X-ray diffraction patterns (a and c), and Pd mean particle size (b and d) of the sintered (pattern 1) and regenerated 5 wt% Pd/20 wt% CeO_2-Al_2O_3 catalysts following oxy-chlorine gas treatment for different time periods: Δt = 0.5 h (pattern 2), 1 h (pattern 3), and 2 h (pattern 4) for two different chlorine-containing gas mixtures: 0.8 vol% Cl_2/18 vol% O_2/He (a and b) and 2.0 vol% Cl_2/18 vol% O_2/He (c and d).

2.3. Catalytic activity measurements

The most efficiently redispersed 5 wt% Pd/γ-Al_2O_3-20 wt% CeO_2 catalyst which exhibited the smallest Pd mean metal particle size (highest dispersion) was tested towards CO oxidation (1 vol% CO/1 vol% O_2/98 vol% He) in the 100–500 °C range. The gas flow-system used for conducting catalytic measurements at 1 atm total pressure, the micro-reactor and the gas analysis system used have been described in detail [32]. The used feed concentration of CO is a representative average value found in the exhaust gas stream at the inlet of a "three-way" catalyst installed in a gasoline-driven car. The amount of catalyst sample used was 30 mg diluted in 120 mg of SiO_2 (150 mg of catalytic bed), and the total volume flow rate was 50 NmL/min. Initially, the catalyst was pretreated in a 20% O_2/He gas mixture at 600 °C for 2 h, and then reduced in pure H_2 at 300 °C for 2 h. The CO conversion versus temperature profile was obtained after applying the "step by step" increase of reaction temperature, and not a reaction temperature ramp (°C/min). The temperature at which 50 and 90% conversion of CO is achieved (T_{50} and T_{90}, respectively) was estimated based on the corresponding CO conversion versus T profile after interpolation. It is also noted that the activity profiles obtained were reproducible within 5–10%.

2.4. In situ DRIFTS NO chemisorption studies

In situ diffuse reflectance infrared Fourier transformed (DRIFT) spectra of NO were collected using a PerkinElmer Spectrum GX I spectrophotometer with a DRIFTS cell (Harrick HVC-DRP). About 30 mg of the powdered sample (KBr/catalyst = 10/1) was packed in the sample holder and pretreated *in situ* in H_2 at 300 °C to ensure that Pd was in the reduced state. Subsequently, the sample was cooled in He flow (50 NmL/min) to room temperature, and the feed was then switched to a 1 vol% NO/He gas mixture (50 NmL/min) for 30 min. A DRIFTS spectrum of dry KBr was taken for IR single-beam background subtraction.

3. Results and discussion

3.1. Pd redispersion efficiency

3.1.1. Effect of oxy-chlorine gas treatment time

Fig. 1a presents powder X-ray diffraction patterns of the sintered supported Pd catalyst (reference catalyst) and of the regenerated ones following oxy-chlorine gas treatments at 500 °C for different times on stream (Δt = 0.5, 1 and 2 h) in 0.8% Cl_2/18% O_2/He gas mixture. Following a given oxy-chlorine gas treatment, the sample was treated in H_2 (1 bar) at 500 °C for 2 h for converting $PdCl_x$ into Pd^0 and removing residual Cl from the catalyst surface (see Section 3.2.1) before XRD measurements.

All samples exhibit 2θ main diffraction peaks at 29°, 33° and 47.5°, which correspond to reflections from the (1 1 1), (2 0 0) and (2 2 0) planes of CeO_2, respectively. Diffraction peaks corresponding to gamma alumina were not observed, indicating the amorphous character of this solid. The presence of alumina primary nanocrystallites (d < 4 nm) escaping XRD detection cannot be ruled out. The efficiency of the oxy-chlorine gas treatment for Pd redispersion was evaluated using the Scherrer equation and the FWHM of diffraction peak at 40° 2θ, the latter corresponding to reflections from the (1 1 1) lattice plane of Pd^0 [35]. The peak recorded at 46.7° corresponds also to Pd^0 (reflections from the (2 0 0) plane), and that

recorded at 47.5° is due to CeO_2. The shape and intensity of the latter peak was found to change with the applied oxy-chlorine gas treatment (see Fig. 1a). As the time in the oxy-chlorine gas treatment increases, the peak at 47.5° becomes smaller and wider, implying a reduction in the Pd crystallite size. A small peak recorded at 36° 2θ (Fig. 1a) appeared only in the case where the treatment of the solid with the 0.8% Cl_2/18% O_2/He gas mixture was applied for 0.5 h on stream. This behaviour implies that this peak corresponds to a metastable phase, which gives rise to a stable one when prolonged treatment and increased Cl_2 concentration were applied. The latter peak corresponds to a PdO_xCl_y phase which is an intermediate in the oxy-chlorine gas induced Pd redispersion process, as will be further discussed in Section 3.2.

As clearly seen in Fig. 1b, a significant decrease of Pd mean particle size is achieved by the increase of oxy-chlorine gas treatment time, which in turn results in an increase of Pd dispersion, D (%), the latter being inversely proportional to d_{Pd} (nm). In particular, the Pd mean particle size of the initially sintered catalyst was found to be 17.3 nm (Δt = 0 h, sintered catalyst), whereas after 1 h and 2 h treatment in the oxy-chlorine gas, the Pd mean particle size drops to 13.8 and 11.5 nm, respectively. No further increase in the oxy-chlorine gas treatment time was investigated. Based on these results, the best oxy-chlorine gas treatment time found was 2 h using the 0.8% Cl_2/18% O_2/He gas mixture at 500 °C.

According to the literature [36,37], the formation of MO_xCl_y surface intermediate seems to be a fundamental step towards M redispersion during the applied oxy-chlorine gas treatment. It could therefore be speculated that further increase in the duration of the latter treatment (kinetic reasons) might have resulted in further improvement of Pd dispersion. It is also evident from the XRD profiles (Fig. 1a) that as the duration of the oxy-chlorine gas treatment increases to Δt = 2 h, the diffractogram is shifted towards slightly higher diffraction angles. Based on the Bragg law ($n\lambda = 2d\sin\theta$), this could be attributed to a slight increase of the unit cell dimensions (lattice expansion) due to a possible incorporation of chlorine and oxygen atoms in the unit cells of CeO_2 and Pd, the former not removed completely by the H_2 treatment applied as evidenced by the XPS studies (see Section 3.2).

After increasing the concentration of Cl_2 in the oxy-chlorine gas mixture, ca. 2 vol% Cl_2/18 vol% O_2/He, the effect of time on stream on the Pd mean particle size appears to be different (compare Fig. 1b and d). A similar dispersion value was obtained after 1 h on stream compared to 2 h on stream when the 0.8 vol% Cl_2/18 vol% O_2/He gas mixture was used. Further increase in the duration of treatment time to 2 h in the former gas mixture results in a negative effect; an increase of Pd mean particle size and a decrease of dispersion were obtained. It is noted that the H_2 reduction step applied at 500 °C before XRD measurements and after the oxy-chlorine gas treatment could have an effect on the behaviour observed (Fig. 1d).

3.1.2. Effect of oxy-chlorine gas mixture composition

Fig. 2a presents XRD patterns of the sintered Pd particles (d_{Pd} = 17.3 nm) and those obtained after an oxy-chlorine gas treatment were applied for a variable chlorine composition (x vol% Cl_2/18 vol% O_2/He, where x = 0.4, 0.8 and 2) at 500 °C for 1 h followed by H_2 treatment at 500 °C for 2 h. The Pd mean particle size obtained as a function of Cl_2 concentration is presented in Fig. 2b. The presence of only 0.4 vol% Cl_2 in the oxy-chlorine gas had only a minor effect on the Pd particle size obtained since a drop from 17.3 nm (sintered) to 16.5 nm was obtained. On the other hand, the presence of 0.8 vol% Cl_2 induced a Pd mean particle size reduction of the order of 20% (17.3–13.8 nm, Fig. 2b), whereas the presence of 2.0 vol% Cl_2 further improved to a significant extent Pd redispersion (17.3–7.5 nm, Fig. 2b). Based on these results, best oxy-chlorine gas treatment conditions were proposed to be those using 2 vol% Cl_2/18 vol% O_2/He at 500 °C for 1 h, resulting in a minimum Pd mean particle size (7.5 nm) and a maximum Pd redispersion. This result is in good agreement with the work of Birgersson et al. [38,39] who reported similar oxy-chlorine gas treatments as effective for Pd redispersion in Pd-Rh commercial TWCs. It is also evident from the given XRD profiles that as the chlorine gas concentration in the oxy-chlorine gas mixture increases, the XRD peaks due to ceria appear to shift towards higher diffraction angles, where the intensity of the peaks is significantly reduced. As stated earlier, this must be attributed to the decrease of the unit cell dimensions (lattice shrinking) due to the formation of some CeOCl (see Section 3.2).

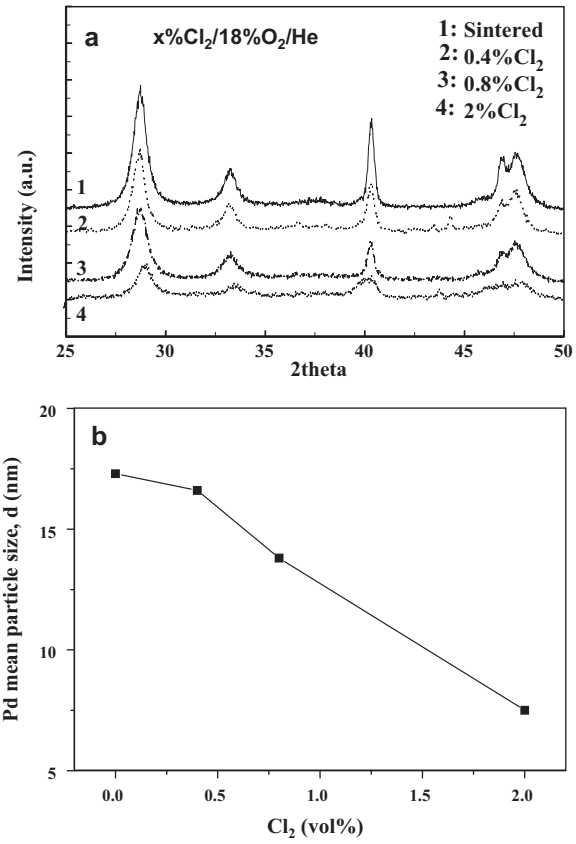

Fig. 2. (a) X-ray diffraction patterns of the sintered (pattern 1), and regenerated 5 wt% Pd/20 wt% CeO_2-Al_2O_3 catalysts using different oxy-chlorine gas treatment compositions: x vol% Cl_2/18 vol% O_2/He (x = 0.4 (pattern 2), 0.8 (pattern 3), and 2 (pattern 4)). (b) Effect of oxy-chlorine gas treatment composition x vol% Cl_2/18 vol% O_2/He (x = 0.4, 0.8 and 2) on the Pd mean particle size (d, nm).

3.1.3. Effect of oxy-chlorine gas treatment temperature

Fig. 3a presents XRD patterns of the sintered Pd catalyst (reference) and those obtained after using the 0.8 vol% Cl_2/18 vol% O_2/He gas mixture for 1 h at different temperatures in the 300–575 °C range. Fig. 3b presents the corresponding Pd mean particle size obtained after the treated catalyst sample was reduced in H_2 at 500 °C for 2 h. It is clearly observed that oxy-chlorine gas treatment at 500 °C for 1 h results in the largest redispersion of Pd, since 57% reduction in the Pd particle size was achieved. At the lowest treatment temperature of 300 °C applied, a Pd mean particle size of 10.7 nm was obtained. The profile of Pd particle size as a function of oxy-chlorine gas treatment temperature (Fig. 3b) is in agreement with other results reported [38–40], where the temperature and composition of Cl-containing gas were found to be important parameters for optimum metal redispersion. It was reported [39] that regeneration of a TWC using an O_2/Cl_2/He gas mixture in the 300–500 °C range led to the highest recovery of catalytic activity,

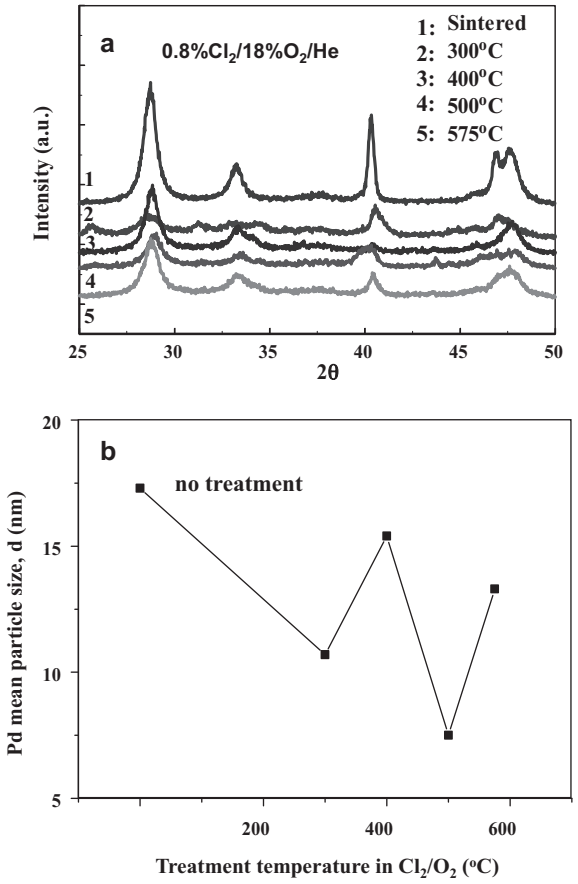

Fig. 3. (a) X-ray diffraction patterns of the sintered (pattern 1), and regenerated 5 wt% Pd/20 wt% CeO_2-Al_2O_3 catalysts after oxy-chlorine gas treatment (0.8 vol% Cl_2/18 vol% O_2/He) at different temperatures: 300 °C (pattern 2), 400 °C (pattern 3), 500 °C (pattern 4), 575 °C (pattern 5). (b) Effect of oxy-chlorine gas treatment temperature on the Pd mean particle size (d, nm). The initial Pd particle size is indicated as "no treatment".

whereas an increase in the oxy-chlorine gas treatment temperature beyond 500 °C resulted in noble metal loss.

3.1.4. *Effect of oxygen/hydrogen gas treatments on Pd redispersion – in situ XRD*

Fig. 4 presents *in situ* X-ray diffraction patterns obtained under a 20 vol% O_2/Ar gas flow over the 5 wt% Pd/20 wt% CeO_2-Al_2O_3 catalyst (calcined *ex situ* in air at 500 °C for 2 h) at 500 °C/1 h (a), 650 °C/1 h (b), 750 °C/1 h (c), 850 °C/30 min (d), 850 °C/1 h (e), and 850 °C/2 h (f). It is shown that decomposition of PdO (peak at $2\theta = 33.8°$) into Pd (peak at $2\theta = 39.9°$) in the presence of the oxygen gas atmosphere becomes discernible by XRD ($d_{Pd} > 3$ nm) at 850 °C. This result is in very good agreement with literature [1,21,23], where depending on the oxygen partial pressure, PdO decomposes in a small temperature range above 800 °C. The Pd mean particle size estimated after the *in situ* oxygen treatment of the sample at 850 °C for 30 min, 1 h and 2 h on stream was 18.0, 20.4 and 18.1 nm, respectively. Following the sample's treatment in 20 vol% O_2/Ar at 850 for 2 h, the sample was then cooled in the oxygen gas mixture first to 750 °C/1 h (g), then to 650 °C/1 h (h), and finally to 500 °C/1 h (i). Subsequently, the solid was purged in Ar flow at 500 °C for 15 min, and then treated in 5 vol% H_2/Ar for 2 h (Fig. 4, spectrum (j)). It is seen that after the sample was cooled to 750 °C in the oxygen gas atmosphere and kept at this temperature for 1 h, the Pd XRD peak disappeared completely, and a PdO phase appeared instead. Further cooling to 500 °C in the oxygen gas atmosphere did not result practically in any change of the PdO mean particle size

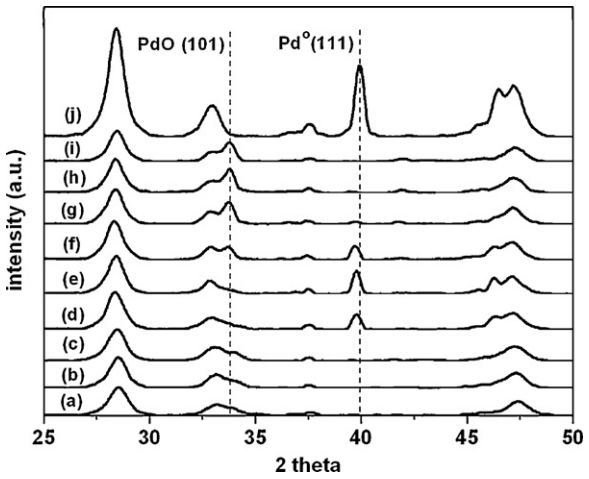

Fig. 4. *In situ* X-ray diffraction patterns obtained under a 20 vol% O_2/Ar gas flow over the 5 wt% Pd/20 wt% CeO_2-Al_2O_3 catalyst (calcined *ex situ* in air at 500 °C for 2 h) at 500 °C/1 h (a); 650 °C/1 h (b); 750 °C/1 h (c); 850 °C/30 min (d); 850 °C/1 h (e); 850 °C/2 h (f). Spectra (g)–(i) were recorded in the sequence after cooling in 20 vol% O_2/Ar gas flow: (g) 750 °C/1 h; (h) 650 °C/1 h; (i) 500 °C/1 h. Following the latter treatment, the solid was purged in Ar flow and then treated in 5 vol% H_2/Ar flow at 500 °C for 1 h (j).

(Fig. 4, spectra (g)–(i)). Treatment of the sample in the hydrogen gas atmosphere resulted in a complete disappearance of PdO XRD peak, and at the same time a Pd peak appeared (Fig. 4, spectrum (j)) corresponding to a Pd mean particle size of 17.0 nm. It is noted the significant overlapping of the diffraction peaks centred at 33° 2θ due to CeO_2, and at 33.8° 2θ due to PdO, result that prevents a direct estimation of the PdO particle size via the Scherrer equation.

In a separate experiment with another solid sample subjected to the same *ex situ* pretreatment previously mentioned, an *in situ* treatment under the 20 vol% O_2/Ar gas flow was made at 850 °C for 8 h, followed by purge in Ar flow. The solid was then cooled in Ar flow to 500 °C or 300 °C and then exposed to a 5 vol% H_2/Ar gas flow for 2 h. Following this treatment, a Pd mean particle size of 16.4 and 14.0 nm, respectively, was estimated (not shown here).

The above described *in situ* XRD results obtained illustrate that redispersion of PdO by high-temperature heating in oxygen gas atmosphere followed by subsequent cooling in the same oxygen gas atmosphere followed by H_2 reduction (300–500 °C) is far considered from being efficient as the alternative oxy-chlorine gas treatment (Fig. 2b). Even though Pd redispersion (spreading of PdO on the support) was reported over a 4 wt% Pd/γ-Al_2O_3 under similar O_2 gas treatments [1], Datye et al. [23] in the case of a 5 wt% Pd/θ-Al_2O_3 solid reported that metallic Pd particles formed at high temperatures (>800 °C) under oxygen gas atmosphere were transformed into PdO polycrystalline domains leading to a decrease in crystallite size but not to redispersion of surface Pd (no increase of surface area of Pd) based on XPS and TEM measurements performed. The different results obtained in the previous studies [1,23] and in the present one are more likely to be related to the different surface tension of Pd and PdO with the alumina and ceria–alumina (present case) supports which control the wetting process [21].

3.2. *Effect of oxy-chlorine gas treatment on catalyst structure*

3.2.1. *X-ray photoelectron spectroscopy (XPS) studies*

Fig. 5 presents X-ray photoelectron core level spectra of Pd 3d after treatment of the solid with 0.8 vol% Cl_2/18 vol% O_2/He gas mixture at 500 °C for 1 h (Fig. 5a), followed by oxidation (20 vol% O_2/He) at 500 °C for 1 h (Fig. 5b), reduction (H_2, 1 bar) at 300 °C for 1 h (Fig. 5c), and further reduction at 500 °C for 1 h (Fig. 5d). All the binding energies and surface atom concentrations (at.%) of

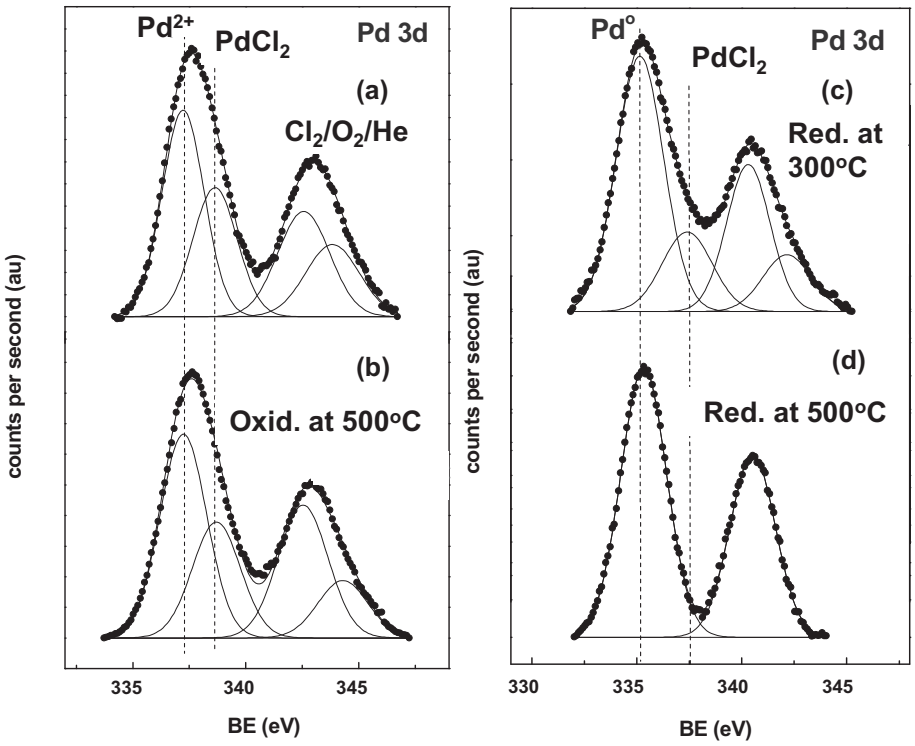

Fig. 5. X-ray photoelectron core level spectra of Pd 3d obtained on a 5 wt% Pd/20 wt% CeO_2-Al_2O_3 catalyst: (a) after oxy-chlorine gas treatment in 0.8 vol% Cl_2/18 vol% O_2/He at 500 °C for 1 h; (b) after oxidation (20 vol% O_2/He, 500 °C, 1 h) following (a); (c) after H_2 reduction (1 bar, 300 °C, 1 h) following (b); and (d) after H_2 reduction (1 bar, 500 °C, 1 h) following (c).

the species of interest are listed in Tables 1 and 2. The Pd XP spectrum can be fitted with two spin–orbit–split doublets [41]. The Pd $3d_{5/2}$ peak located at ~335.7 eV is attributed to Pd^0, whereas that at ~337.5 eV to Pd^{2+} (palladium oxide) [42]. The XP spectrum of Ce (not presented) was more complicated due to the mixing of Ce 4f and O 2p states [43]. As seen in Fig. 5a, after the solid was treated in the 0.8% Cl_2/18% O_2/He gas mixture at 500 °C for 1 h, Pd is converted to PdO (Pd^{2+}) and $PdCl_2$. Further treatment of the solid in 20 vol% O_2/He at 500 °C for 1 h (Fig. 5b) followed by H_2 treatment at 300 °C for 1 h (Fig. 5c) was proved not efficient for a large removal of chlorine ions from the catalyst surface. However, after H_2 treatment at 500 °C for 1 h (Fig. 5d) reduction of palladium ($PdCl_2$) to Pd^0 is practically complete, result that led to higher OSC values and better catalytic performance towards CO oxidation as will be shown in Section 3.3.

Based on the surface % atom composition obtained from the XPS studies (Table 2), it is noted that part of chlorine ions was accommodated on the CeO_2-containing support. At the end of the above-mentioned oxidation/reduction treatments applied, Ce concentration was found to be 4.4 at.% (see footnote (e) in Table 2), whereas after oxy-chlorine gas treatment this was found to be 5.6 at.%. In addition, Cl surface concentration was found to be 4.7 at.% after H_2 reduction at 500 °C for 1 h compared to 6.5 at.% after oxy-chlorine gas treatment. It is also known that chlorine arising from $PdCl_2$ can react with CeO_2 in the 500–600 °C range, when these two phases are in intimate contact, thus forming CeOCl, which stabilizes cerium in the Ce^{3+} state. It was found that the latter compound is stable even after reduction in H_2 at 700 °C [44]. Also, based on the results of Table 2 it is observed that in all cases Pd surface concentration decreases following reduction, an opposite

Table 1
XPS binding energies (eV) of core electrons of Al 2p, Ce 3d, Cl 2p and Pd 3d for the 5 wt% Pd/20 wt% CeO_2-Al_2O_3 catalyst subjected to successive oxidation/reduction treatments, following oxy-chlorine gas treatment.[a]

Pretreatment	Al 2p (eV)	Ce $3d_{5/2}$ (eV)	Cl $2p_{3/2}$ (eV)	Pd $3d_{5/2}$ (eV)
Oxy-chlorination[a]	74.5	882.5	198.8	337.2 (60) 338.6 (40)
Reduction[b]	74.5	882.2	198.8	335.1 (75) 337.4 (25)
Oxidation[c]	74.5	882.3	198.7	337.2 (63) 338.7 (37)
Reduction[d]	74.5	882.1	198.7	335.2 (78) 337.4 (22)
Oxidation[c]	74.5	882.4	198.7	337.4 (67) 338.8 (33)
Reduction[e]	74.5	882.2	198.8	335.1 (100)

[a] Use of 0.8 vol% Cl_2/18 vol% O_2/He at 500 °C for 1 h.
[b] Reduction in H_2 at 300 °C for 1 h following oxy-chlorine gas treatment.
[c] Oxidation (20 vol% O_2/He, 500 °C, 1 h) following pre-treatment as in footnote (b).
[d] Reduction in H_2 at 500 °C for 0.5 h following pre-treatment as in footnote (c).
[e] Reduction in H_2 at 500 °C for 1 h following pre-treatment as in footnote (d).

Table 2
Surface % atom composition (Al, Ce, Cl, Pd) of 5 wt% Pd/20 wt% CeO_2-Al_2O_3 catalysts subjected to successive reduction/oxidation treatments, following oxy-chlorine gas treatment.[a]

Pretreatment	Al (at.%)	Ce (at.%)	Cl (at.%)	Pd (at.%)
Oxy-chlorination[a]	84.9	5.6	6.5	3.0
Reduction[b]	84.4	6.1	6.0	3.5
Oxidation[c]	83.3	5.7	6.3	4.7
Reduction[d]	85.7	5.8	5.0	3.5
Oxidation[c]	85.8	4.5	5.4	4.3
Reduction[e]	87.8	4.4	4.7	3.1

[a] Use of 0.8 vol% Cl_2/18 vol% O_2/He at 500 °C for 1 h.
[b] Reduction in H_2 at 300 °C for 1 h following oxy-chlorine gas treatment.
[c] Oxidation (20 vol% O_2/He, 500 °C, 1 h) following pre-treatment as in footnote (b).
[d] Reduction in H_2 at 500 °C for 0.5 h following pre-treatment as in footnote (c).
[e] Reduction in H_2 at 500 °C for 1 h following pre-treatment as in footnote (d).

behaviour to that seen in the case of oxidation treatment. This might be due to partial decoration of metal Pd particles with reduced ceria in agreement with the work of Bernal et al. [45]. This decoration effect is in harmony with the increase of Ce surface % atom concentration following the first two reduction treatments (Table 2).

Scheme 1 presents the suggested process steps of redispersion of a CeO_2-Al_2O_3-supported Pd catalyst after applying the oxy-chlorine gas treatment followed by hydrogen reduction according to the findings of the present work. Compounds such as PdO, $PdCl_2$ and PdO_xCl_y are formed as intermediates after treatment in Cl_2/O_2/He gas mixture is applied. H_2 reduction temperature is suggested to control the concentration of residual Cl on the surface of both the support and the active metal. Thus, following reduction at 300 °C, residual Cl on Pd is found, whereas H_2 reduction at 500 °C leads to Pd^0 (Fig. 5d). Different mechanistic pathways have been proposed in the literature [36,37] for metal redispersion, such as metal oxide volatilization, atoms/molecular species migration to another area of support, and particles break-up into two or more particles (Scheme 1a–c). The mechanism presented in Scheme 1a cannot be excluded as a possible redispersion path in the case of H_2 reduction at 300 °C, whereas mechanisms depicted in Scheme 1b and c are possible to favour Pd redispersion in the case where hydrogen reduction is performed at 500 °C.

3.2.2. HR-TEM studies

HR-TEM studies were performed in order to directly evaluate the Pd mean particle size and compare it with that estimated from the XRD studies (Figs. 1–3). Fig. 6 presents a HR-TEM micrograph obtained over the 5 wt% Pd/20 wt% CeO_2-Al_2O_3 catalyst after treatment in the 2 vol% Cl_2/18 vol% O_2/He gas mixture at 500 °C for 1 h, where the latter process was found to provide best results in terms of Pd redispersion. The dark areas in the image represent Pd metal particles, where after counting about 200 particles, a mean Pd particle size of 8.2 nm was estimated, in good agreement with the XRD results (Sections 3.1.2 and 3.1.3).

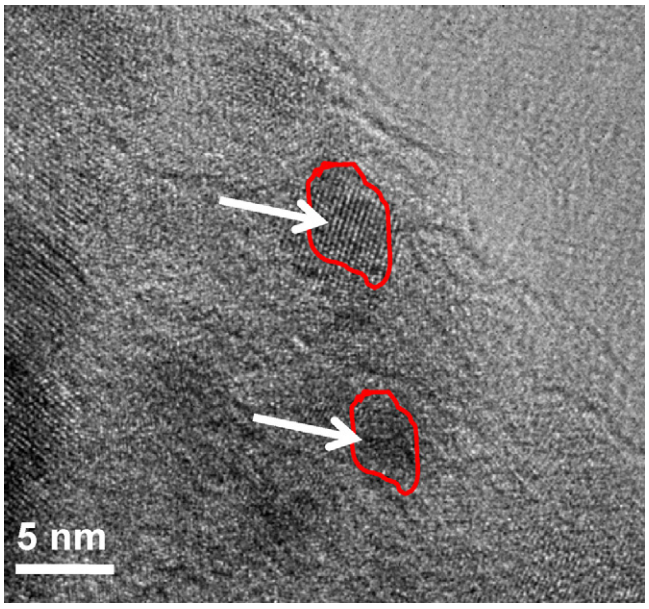

Fig. 6. HR-TEM image of a 5 wt% Pd/20 wt% CeO_2-Al_2O_3 catalyst following oxy-chlorine gas treatment under optimum conditions: 2 vol% Cl_2/18 vol% O_2/He at 500 °C for 1 h.

3.2.3. H_2-TPR studies

Fig. 7 presents H_2-TPR traces obtained over the sintered and redispersed Pd catalysts, following the oxy-chlorine gas treatment in 2 vol% Cl_2/18 vol% O_2/He gas mixture at 500 °C for 1 h. Both catalysts exhibit a main reduction peak at 130 °C, which is attributed to reduction of Pd^{2+} (PdO) to metallic Pd^0 [46–48], followed by a second smaller reduction peak at higher temperatures (~200–220 °C). In particular, for the reference (sintered) catalyst the second small peak appears at 200 °C which becomes broader

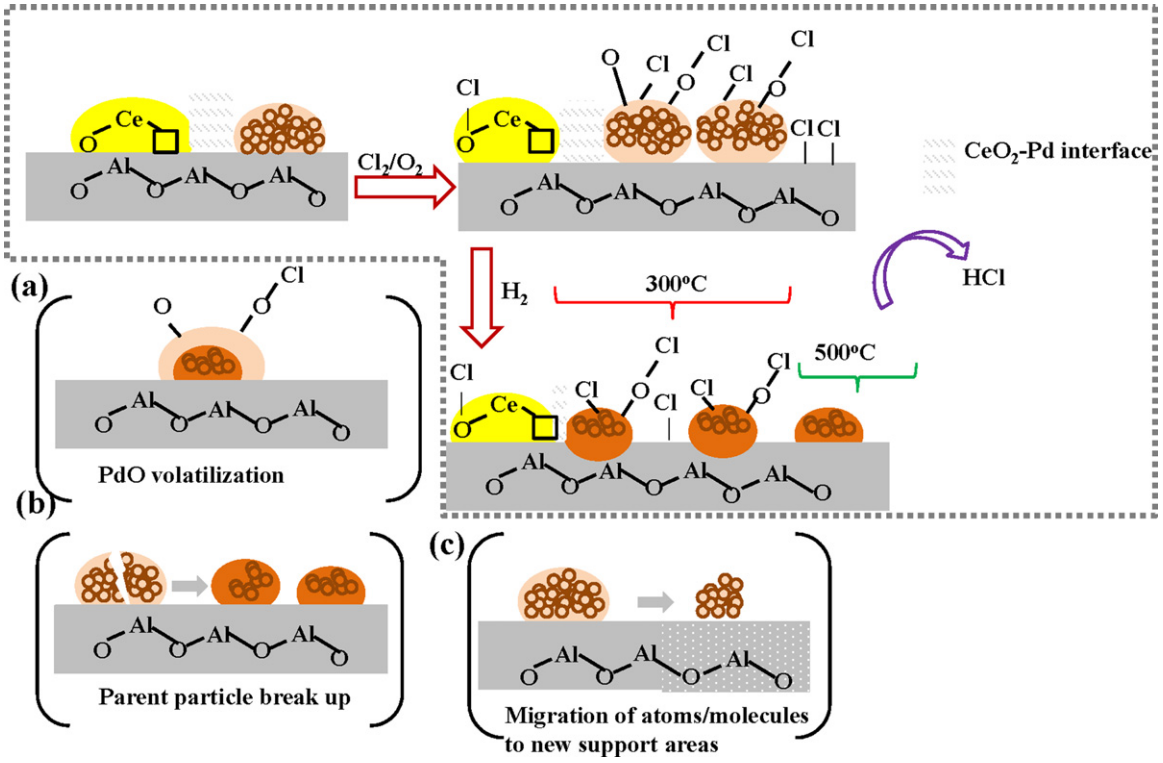

Scheme 1. Oxy-chlorination gas treatment followed by H_2 reduction and proposed redispersion mechanism over CeO_2-Al_2O_3-supported Pd catalysts.

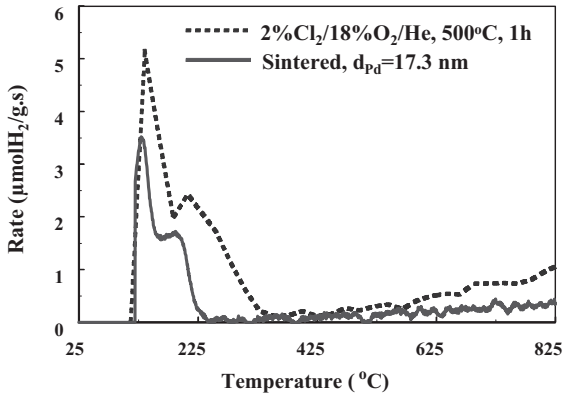

Fig. 7. H_2-TPR profiles obtained over a 5 wt% Pd/20 wt% CeO_2-Al_2O_3 catalyst sintered (d_{Pd} = 17.3 nm) and redispersed (d_{Pd} = 7.5 nm) using a 2 vol% Cl_2/18 vol% O_2/He gas mixture at 500 °C for 1 h.

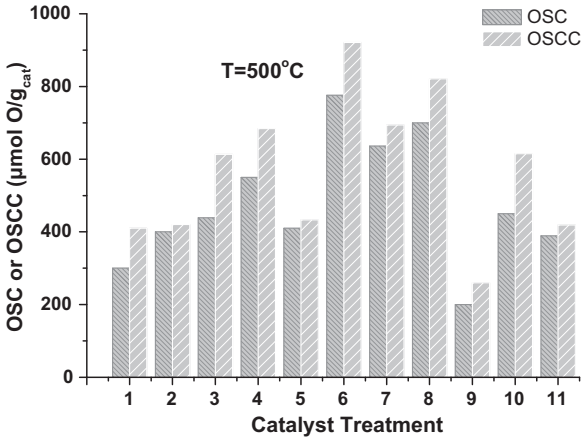

Fig. 8. OSC and OSCC quantities (μmol O/g_{cat}) measured at 500 °C over the 5 wt% Pd/20 wt% CeO_2-Al_2O_3 catalyst following different oxy-chlorine gas treatments (Table 3).

(200–400 °C, $T_M \sim 220$ °C) after the catalyst was treated in the 2% Cl_2/18% O_2/He gas mixture. According to previous studies [49,50], H_2-TPR peaks in the 200–400 °C range are attributed to the reduction of noble metal oxides which are in close proximity and intimate contact with CeO_2 nanocrystallites (e.g., Pd–O–Ce species). The very broad H_2-TPR trace appeared in the 450–825 °C range corresponds to reduction of subsurface/bulk oxygen (e.g., O^{n-}) of CeO_2. Fig. 7 shows that in the case of catalyst treatment in the oxy-chlorine gas mixture the intensity of the first peak (T_M = 130 °C) becomes larger compared to that observed in the non-treated sintered Pd-based catalyst. This result is in good agreement with the work of Daley et al. [51], who investigated the redispersion of noble metals in the Rh-Pd/$Ce_xZr_{1-x}O_2$-Al_2O_3 catalyst following a dichloro-propane (DCP)/air gas mixture treatment.

The significant increase of hydrogen consumption rate at low temperatures (Fig. 7) is correlated well with the increase in the number of exposed Pd surface atoms per gram of catalyst. Due to Pd particle size reduction, an increase in the interfacial perimeter between Pd and CeO_2 (OSC material) is achieved, and this could explain the increase in the magnitude of the second TPR peak recorded in the 200–400 °C range. It was reported [51] that reduction of compounds formed between Pd, CeO_2 and Al_2O_3 can be realized in the 200–400 °C range, which is highly favoured over small noble metal particles [49,50,52]. As will be illustrated in Section 3.3.1, the present H_2-TPR studies support the OSC measurements performed according to which Pd redispersion has increased significantly the OSC of the catalyst, in agreement with the work of Daley et al. [51], who reported that the recovery of OSC over Pd-Rh/$Ce_xZr_{1-x}O_2$-Al_2O_3 catalysts after treatment with DCP/air gas mixtures can be attributed to the increase in the interactions between noble metal and the oxide support.

3.3. Effect of oxy-chlorine gas treatment on catalyst activity

3.3.1. OSC measurements

Fig. 8 presents OSC and OSCC values (μmol O/g_{cat}) obtained over the 5 wt% Pd/20 wt% CeO_2-Al_2O_3 catalyst at T_{OSC} = 500 °C following different oxy-chlorine gas treatment conditions (see Table 3). For comparison purposes, OSC values of the sintered catalyst (treatment no. 1, Fig. 8) are also presented. It is seen (Fig. 8 and Table 3) that most of the oxy-chlorine gas treatments applied resulted in a significant increase of OSC and OSCC of the treated catalysts when compared to the values obtained for the sintered catalyst. The oxy-chlorine gas treatment in 2 vol% Cl_2/18 vol% O_2/He at 500 °C for 1 h (catalyst treatment no. 6, Fig. 8) led to the highest OSC obtained among the other treatments applied. It is important to mention here that the ratio of OSC and OSCC (T_{OSC} = 500 °C) quantities for catalyst treatment no. 6 to that of no. 1 was found to be ~2.6 and ~2.2, respectively. This result is consistent with the fact that catalyst treatment with 2 vol% Cl_2/18 vol% O_2/He at 500 °C for 1 h gave the smallest Pd mean particle size (ca. 7.5 nm).

It is pointed out that the oxy-chlorine gas treatment could block the OSC process since the presence of Cl^- ions can lead to the formation of Cl-containing phases/species, such as CeOCl [44],

Table 3
OSC and OSCC quantities (μmol O/g_{cat}) measured over the 5 wt% Pd/20 wt% CeO_2-Al_2O_3 catalysts following different oxy-chlorine gas treatments.

	Catalyst treatment	T_{OSC} (°C)	OSC_{H_2} (μmol O/g)	$OSCC_{H_2}$ (μmol O/g)
1	Reference catalyst	500	300	410
		700	500	654
		850	781	856
2	0.8% Cl_2/18% O_2/He,	500	400	420
	500 °C, 30 min	700	544	778
		850	780	922
3	0.8% Cl_2/18%	500	439	613
	O_2/He, 500 °C, 1 h	700	623	799
		850	820	718
4	0.8% Cl_2/18%	500	550	684
	O_2/He, 500 °C, 2 h	700	699	935
		850	744	886
5	2% Cl_2/18% O_2/He,	500	410	433
	500 °C, 30 min	700	457	580
		850	667	761
6	2% Cl_2/18% O_2/He,	500	776	921
	500 °C, 1 h	700	920	1252
		850	1119	1348
7	2% Cl_2/18% O_2/He,	500	636	694
	500 °C, 2 h	700	781	848
		850	867	1104
8	2% Cl_2/18% O_2/He,	500	700	821
	300 °C, 1 h	700	757	954
		850	1046	1106
9	2% Cl_2/18% O_2/He,	500	200	260
	400 °C, 1 h	700	500	560
		850	754	824
10	2% Cl_2/18% O_2/He,	500	450	615
	575 °C, 1 h	700	657	826
		850	825	987
11	0.4% Cl_2/18%	500	389	419
	O_2/He, 500 °C, 1 h	700	587	600
		850	600	620

which lock the Ce^{4+}/Ce^{3+} redox couple [52]. According to the XPS results (Fig. 5), application of an oxy-chlorine gas treatment on the present supported Pd catalyst at 300 °C for 1 h resulted in significant amounts of catalyst surface residual Cl. The latter implies the formation of a strong bond with Ce^{3+}, leading to weaker Pd–Ce interactions [53]. Also, it was found [54] that Cl^- ions hinder the development of highly dispersed Pd. Based on the surface % atom concentrations obtained in the XPS studies (Table 2), the different conditions applied in each of the oxy-chlorine gas treatments caused cerium migration towards the inner or outer surface layers. This could form nano-scale heterogeneities, e.g., Ce-rich domains, which could facilitate OSC. Differences in the size of these Ce-rich domains could also explain OSC variations. Mamontov et al. [55] reported that, in the case of $Ce_{0.7}Zr_{0.3}O_2$ solid solution, a decrease in the size of such a domain from 30 to 25 Å induced a 20% increase in the interfacial area, which boosts oxygen population in the proximity of the metal–support interface, thus increase in OSC.

It is also useful to mention here that catalysts treated in 2 vol% Cl_2/18 vol% O_2/He at 500 °C for 2 h and 2 vol% Cl_2/18 vol% O_2/He at 300 °C for 1 h present high OSC and OSCC in comparison with all the other oxy-chlorine gas treatments applied (Table 3). This can be explained by considering the relatively small Pd particle size achieved following these particular treatments, namely, 10.9 and 10.7 nm, respectively. Daley et al. [51] reported that after using DCP/air for regeneration of the Pd-Rh/$Ce_xZr_{1-x}O_2$-Al_2O_3 catalyst, an increase in OSC and OSCC in the 400–850 °C range was obtained, mainly due to noble metal redispersion. It was also reported [34,56,57] that the OSC of a metal supported catalyst is greatly affected by the metal particle size, since oxygen diffusion from the CeO_2 support through metal–support interface is an important step for the functioning of the OSC process. Also, the fact that the crystallite size of both Pd and CeO_2 is influenced by the gas treatment temperature, this could partly provide a reasonable explanation for the different OSC and OSCC values obtained following treatments under 2 vol% Cl_2/18 vol% O_2/He for 1 h at different temperatures (300, 400 and 575 °C).

It is to be emphasized that the oxy-chlorine gas treatment conditions applied, which led to the enhancement of OSC, were those performed using a high chlorine-containing gas composition. Chlorine-induced modifications in the Pd-CeO_2 vicinity have been reported to trigger oxygen activation at the interface [58,59], thus influencing the rate of oxygen back-spillover. According to Arteaga et al. [60], an oxy-chlorine gas treatment applied on Pt-based catalysts led to large crystallites of Pt covered with O-adatoms. The formations of Cl-adatoms or oxy-chloro-Pt complexes on the surface of Pt particles or in the alumina support were not ruled out. The different oxy-chlorine gas treatments applied in the present study for the Pd-based catalysts might be proposed to have led to a different extent of formation of such type of complex compounds, and also to a different kinetics of their decomposition. All these factors could drive the variation in Pd spreading (redispersion) onto the present CeO_2–Al_2O_3 support.

Based on the above considerations, and after comparing the H_2-TPR profiles (Fig. 7) and the OSC reported in Table 3, it could be stated that the main reason for the observed increase in OSC after an oxy-chlorine gas treatment was applied followed by H_2 reduction is the increase in the metal (Pd)–ceria–alumina interactions, due to the reduction occurred in the Pd crystallite size. The latter resulted in turn in the increase of the interfacial perimeter.

3.3.2. CO oxidation catalytic studies

To determine whether Pd redispersion does lead to an increased catalytic performance for the treated 5 wt% Pd/20 wt% CeO_2-Al_2O_3 catalyst compared to the non-treated sintered one (d_{Pd} ~17.3 nm), the CO oxidation reaction was tested. Fig. 9 reports light-off

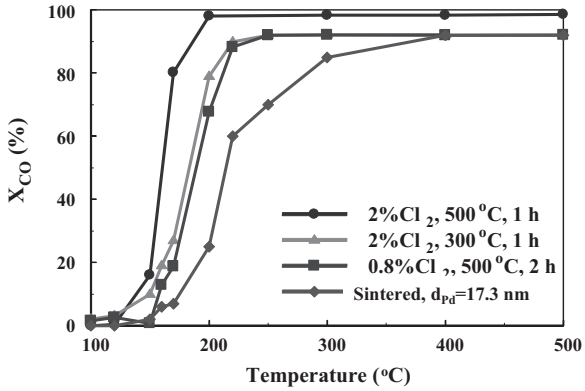

Fig. 9. Light-off CO conversion (X_{CO}) profile obtained for the CO oxidation reaction (1 vol% CO/1 vol% O_2/He) in the 100–500 °C range over the aged and regenerated 5 wt% Pd/20 wt% CeO_2-Al_2O_3 catalyst under different oxy-chlorine gas treatments.

catalytic activity profiles in the 100–500 °C range for three different oxy-chlorine gas treatments. It is seen that the activity of the catalyst in the 150–300 °C range following oxy-chlorine gas treatment is significantly improved compared to the one obtained for the non-treated sintered catalyst. In particular, it is pointed out the performance of the catalyst treated in 2 vol% Cl_2/18 vol% O_2/He gas mixture at 500 °C for 1 h, which resulted in a significant decrease of Pd mean particle size, from 17.3 to 7.5 nm (Fig. 2). For this specific treatment, the T_{50} dropped by ~50 °C, whereas the T_{90} by ~150 °C (Fig. 9). These important catalytic results are in good agreement with the XRD, OSC and H_2-TPR studies previously presented and discussed. It should be stated at this point that the treatment of the present Pd-based catalyst with Cl_2/O_2/He gas mixtures resulted in a definite increase of available Pd active sites for CO chemisorption based on the remarkable Pd redispersion achieved. The increase of OSC observed after applying this oxy-chlorine gas treatment (Fig. 8 and Table 3) must be attributed to Pd redispersion as strongly supported by the XRD and HR-TEM studies. The latter leads to the increase in the rate of labile oxygen back-spillover process. Birgersson et al. [38,39] reported also an increase of catalytic activity in CO oxidation due to redispersion of Pd in a Pd-Rh-based commercial TWC after applying the oxy-chlorine gas treatment.

According to the fundamental mechanistic steps of CO oxidation at temperatures lower than 500 °C over supported metal catalysts, this takes place mainly on the active metal. However, oxygen species of reducible supports (e.g., ceria, lanthana, etc.) participate in the reaction path by a surface diffusion process towards the metal surface (oxygen back spillover) [34,57,61]:

$$CeO_2 \rightarrow 2xCe_{Ce}' + (1-2x)Ce_{Ce} + xV_o + (2-x)O_o + xO \quad (1)$$

$$O + s \rightarrow O\text{-}s \quad (2)$$

$$CO(g) + s \rightarrow CO\text{-}s \quad (3)$$

$$CO\text{-}s + O\text{-}s \rightarrow CO_2\text{-}s + s \quad (4)$$

$$CO_2\text{-}s \rightarrow CO_2(g) + s \quad (5)$$

where Eq. (1) presents the formation of oxygen vacancies (V_o), Ce_{Ce}' stands for the formation of Ce^{3+} ions, Ce_{Ce} stands for Ce^{4+}, and O is a labile oxygen. Eq. (2) presents the chemisorption step of support labile oxygen onto Pd sites (denoted as s), Eq. (3) the chemisorption step of CO onto the metal surface, and Eqs. (4) and (5) the formation of CO_2 and its desorption step, respectively, on the metal surface. It was reported [62,63] that when Pd is impregnated as cationic precursor species onto a ceria-based support, it has the tendency to disperse over the ceria-rich (as opposed to alumina-rich) areas of support after calcination. As a consequence, thermal aging of these catalysts can be linked to the loss of interactions between the Pd

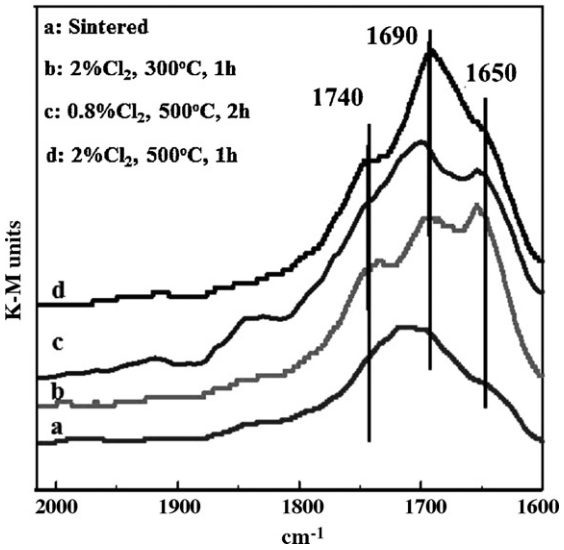

Fig. 10. *In situ* DRIFTS spectra obtained over the 5 wt% Pd/20 wt% CeO_2-Al_2O_3 catalyst in the 2000–1600 cm^{-1} range as sintered and after following different oxy-chlorine gas treatments.

and CeO_2 promoter after sintering [60,64]. The latter leads to the decline in the rate of oxygen back-spillover.

Another important aspect of the oxy-chlorine gas treatment is the Cl-induced modification of support's Brönsted acidity. According to the XPS results (Table 2), residual Cl^- was measured. It would be expected that the presence of chlorine could alter the electronic properties of Pd and reduce its chemisorptive properties towards CO and O, according to the work of Gao et al. [54], who reported that Cl^- ions hinder Pd dispersion in the case of alumina-supported Pd catalysts. For the CO oxidation reaction, weak structure sensitivity for small Pd particles has been reported [65]. This sensitivity is, however, more intense in the case of easily reducible supports, such as CeO_2. The presence of Cl changes the support's Brönsted acidity, and this could be a possible reason for some modification of the Pd/CeO_2–Al_2O_3 interface [65]. Also, Kili and Normand [66] reported that Cl induces a modification of the Pd–CeO_2 interface through formation of a bridged Pd–Cl^-–Ce^{3+} species that enhances dissociation of hydrocarbons. It was reported [67] that due to this kind of modification, Pd–CeO_2 interface provides some additional structure sensitivity to the CO oxidation reaction and also to the very specific geometrical details of Pd metal (exposed planes, O- and/or Cl-adatoms). On the other hand, Oran and Uner [68] reported that chlorine ions preferentially occupy catalytic sites that are not responsible for CO oxidation, where Cl^- ions occupy corner and edge sites which exhibit electron deficient character. Furthermore, it was reported [68,69] that CO oxidation takes place over surfaces of planar geometry. Therefore, as oxy-chlorine gas treatment becomes more severe, the ultimate effectiveness of such a treatment is accomplished, and at the same time residual Cl^- does not inhibit the rate of CO oxidation.

3.4. *In situ* DRIFTS NO chemisorptions studies

Fig. 10 presents *in situ* DRIFTS spectra recorded in the 2000–1600 cm^{-1} range over three samples exposed to different oxy-chlorine gas treatments, as well as over the reference catalyst (sintered, d_{Pd} = 17.3 nm) after 30 min of NO adsorption at 25 °C. The IR band at 1740 cm^{-1} corresponds to linear adsorbed NO on Pd^0 [70–74], that at 1690 cm^{-1} to bent Pd–NO^-, whereas that at 1650 cm^{-1} to linear Pd–NO^- on the Pd^0 surface [70]. It is interesting to note that NO adsorbed on Pd^{2+} was not observed. The latter result was rather expected since strong NO adsorption takes place on reduced Pd surface, although NO can cause oxidation of Pd to Pd^{n+} during adsorption at 25 °C leading to N_2O formation [75]; the latter, if occurred, was very minor.

It is observed that all IR bands corresponding to NO chemisorption on Pd^0 appear to significantly increase after the oxy-chlorine gas treatment was applied. Haneda et al. [71] have studied the NO chemisorption on Pd/Al_2O_3 and reported that population of NO adsorbed species is strongly related to the number of exposed Pd sites. In the present work (Fig. 10), the surface concentration of different adsorbed species, namely: bent Pd–NO^-, linear Pd–NO^- and Pd–NO were found to be different for the samples treated in different Cl_2/O_2 gas composition and temperature. In particular, the catalyst treated in 2 vol% Cl_2/18 vol% O_2/He at 500 °C for 1 h, which is the catalyst sample that showed the largest Pd redispersion, exhibits the largest integral band intensity at 1690 cm^{-1} (bent Pd–NO^- species). It was reported [76] that formation of bent adsorbed NO species is greatly facilitated on sites having specific geometry, namely, a step or terrace site. For the present 5 wt% Pd/20 wt% CeO_2-Al_2O_3 solid, a facile reaction step of adsorbed NO on Pd with CeO_2-based oxygen anion vacancies pair site could be facilitated, resulting in the weakening of N–O bond. This might be enhanced due to the presence of Pd particles of small size [67].

4. Conclusions

The following conclusions can be derived from the results of the present work:

(a) Oxy-chlorine gas treatment followed by H_2 reduction at 500 °C was found to be a very effective tool for a significant redispersion of Pd over a 5 wt% Pd/20 wt% CeO_2-Al_2O_3 catalyst, resulting in a significant enhancement of catalytic activity towards CO oxidation and also in NO chemisorption (increase of surface Pd sites).

(b) The effect of different experimental parameters used in the oxy-chlorine gas treatment, namely: time on stream, temperature, and chlorine concentration in the reactive gas mixture (Cl_2/O_2/He) was critically evaluated in order to select best conditions for Pd redispersion and catalytic performance (CO oxidation). Among the conditions applied for Pd redispersion, oxy-chlorination at 500 °C for 1 h under a 2 vol% Cl_2/18 vol% O_2/He gas mixture was the best in terms of Pd redispersion and catalytic performance. On the other hand, oxygen treatment at high temperatures (500–850 °C) followed by H_2 reduction at 500 °C did not result in any significant reduction in the size of Pd particles over the present 5 wt% Pd/20 wt% CeO_2-Al_2O_3 catalyst.

(c) The surface % atom concentration of Pd, Cl, Ce and Al catalyst's constituents measured by XPS after oxy-chlorine gas treatment and successive oxidation/reduction treatments revealed that reduction (H_2, 1 bar) at 500 °C is necessary to effectively remove residual Cl from the Pd surface. It was also found that this reduction step causes a decline in surface Pd concentration with a concomitant Ce surface concentration increase. This could be attributed to some partial decoration of Pd crystallites with ceria moieties.

(d) Following different oxy-chlorine gas treatments, OSC and OSCC were significantly increased due to the Cl-induced alteration of Pd–support interface, Pd redispersion, and support modification. All these factors led to an enhancement in the rate of oxygen back-spillover, thus in the rate of CO oxidation.

(e) The oxy-chlorine gas treatment applied over the 5 wt% Pd/20 wt% CeO_2-Al_2O_3 catalyst resulted in a significant enhancement in the rate of CO oxidation compared to that observed in the sintered catalyst. In particular, a drop of X_{50}

and X_{90} by 50 and 150 °C, respectively, was obtained. This result coincides with an increase in the CO uptake (Pd phase contribution) and a faster rate of oxygen back spillover (Pd–ceria support contribution). The redispersion of Pd (particles of reduced size), and the subsequent increase in the concentration of low-coordinated sites, where CO chemisorption is favoured, seems to play a decisive role towards the CO oxidation.

(f) The aged catalyst and the oxy-chlorine gas treated ones were studied by *in situ* DRIFTS towards NO chemisorption. Linear adsorbed NO, bent Pd–NO^- and linear Pd–NO^- species were clearly identified. The oxy-chlorine gas treatment was found to largely influence the integral band intensity of bend Pd–NO^-, result that could be directly linked with the reduction in the size of Pd particles that cause an increase in the concentration of surface Pd sites, along with electronic and geometrical changes in the Pd–support interface.

Acknowledgements

The financial support by the European Union (contract no. G5RD-CT-2000-00376) and the Research Committee of the University of Cyprus is gratefully acknowledged. Professor José-Luis Garcia Fierro (Institute of Catalysis and Petrochemistry-CSIC, Madrid, Spain) is deeply acknowledged for performing the XPS and HR-TEM studies.

References

[1] R.J. Farrauto, M.C. Hobson, T. Kennelly, E.M. Waterman, Appl. Catal. A: Gen. 81 (1992) 227.
[2] F. Yin, S. Ji, P. Wu, F. Zhao, H. Liu, C. Li, ChemSusChem 1 (2008) 311.
[3] G. Pecchi, P. Reyes, R. Zamora, T. López, R. Gómez, J. Chem. Technol. Biotechnol. 80 (2005) 268.
[4] G. Pecchi, P. Reyes, T. López, R. Gómez, J. Non-Cryst. Solids 345–346 (2004) 624.
[5] G. Pecchi, P. Reyes, I. Concha, J.L.G. Fierro, J. Catal. 179 (1998) 309.
[6] F. Arosio, S. Colussi, G. Groppi, A. Trovarelli, Top. Catal. 42–43 (2007) 405.
[7] P. Forzatti, Catal. Today 83 (2003) 3.
[8] S. Specchia, E. Finocchio, G. Busca, P. Palmisano, V. Specchia, J. Catal. 263 (2009) 134.
[9] Z.R. Ismagilov, M.A. Kerzhentsev, T.L. Susharina, Russ. Chem. Rev. 59 (1990) 973.
[10] L.S.F. Feio, C.E. Hori, S. Damyanova, F.B. Noronha, W.H. Cassinelli, C.M.P. Marques, J.M.C. Bueno, Appl. Catal. A: Gen. 316 (2007) 107.
[11] R. Cracium, W. Daniell, H. Knözinger, Appl. Catal. A: Gen. 230 (2002) 153.
[12] W.L.S. Faria, L.C. Dieguez, M. Schmal, Appl. Catal. B: Environ. 85 (2008) 77.
[13] A.L. Guimarães, L.C. Dieguez, M. Schmal, J. Phys. Chem. B 107 (2003) 4311.
[14] N.L. Wieder, M. Cargnello, K. Bakhmutsky, T. Montini, P. Fornasiero, R.J. Gorte, J. Phys. Chem. C 115 (2011) 915.
[15] J.C. Brown, E. Gulari, Catal. Commun. 5 (2004) 431.
[16] X. Lu, L. Luo, X. Chen, React. Kinet. Catal. Lett. 94 (2008) 35.
[17] J. Noh, O.-B. Yang, D.H. Kim, S.I. Woo, Catal. Today 53 (1999) 575.
[18] H.S. Gandhi, G.W. Graham, R.W. McCabe, J. Catal. 216 (2003) 433.
[19] I. Sushumna, E. Ruckenstein, J. Catal. 108 (1987) 77.
[20] F. Le Normand, A. Borgna, T.F. Garetto, C.R. Apesteguia, B. Moraweck, J. Phys. Chem. 100 (1996) 9068.
[21] J.J. Chen, E. Ruckenstein, J. Phys. Chem. 85 (1981) 1606.
[22] J.J. Chen, E. Ruckenstein, J. Catal. 69 (1981) 254.
[23] A.K. Datye, J. Bravo, T.R. Nelson, P. Atanasova, M. Lyubovsky, L. Pfefferle, Appl. Catal. A: Gen. 198 (2000) 179.
[24] M.M. Wolf, H. Zhu, W.H. Green, G.S. Jackson, Appl. Catal. A: Gen. 244 (2003) 323.
[25] M.J. D'Aniello, D.R. Monroe, C.J. Carr, M.H. Krueger, J. Catal. 109 (1988) 407.
[26] S. Kim, M.J. D'Aniello, Appl. Catal. 56 (1989) 45.
[27] B.R. Powell, Y. Chen, Appl. Catal. 53 (1989) 233.
[28] V. Meeyoo, D.L. Trimm, N.W. Cant, Appl. Catal. B: Environ. 16 (1998) L101.
[29] G.C. Joy, F.S. Molinaro, E.H. Homeier, SAE Technical Paper Series 852099, 1985.
[30] H. Birgersson, M. Boutonnet, F. Kingstedt, D.Y. Marzin, P. Stefanov, A. Naydenov, Appl. Catal. B: Environ. 65 (2006) 93.
[31] J.A. Anderson, R.A. Daley, S.Y. Christou, A.M. Efstathiou, Appl. Catal. B: Environ. 64 (2006) 189.
[32] C.N. Costa, T. Anastasiadou, A.M. Efstathiou, J. Catal. 194 (2000) 250.
[33] H.C. Yao, Y.F. Yu Yao, J. Catal. 86 (1984) 254.
[34] P.S. Lambrou, C.N. Costa, S.Y. Christou, A.M. Efstathiou, Appl. Catal. B: Environ. 54 (2004) 237.
[35] J. Wang, M. Shen, Y. An, J. Wang, Catal. Commun. 10 (2008) 103.
[36] T.J. Lee, Y.G. Kim, J. Catal. 90 (1984) 279.
[37] F.L. Normand, A. Borgna, T.F. Garetto, C.R. Apesteguía, B. Moraweck, J. Phys. Chem. 100 (1996) 9068.
[38] H. Birgersson, M. Boutonnet, S.G. Järas, L. Eriksson, Top. Catal. 30 (2004) 433.
[39] H. Birgersson, L. Eriksson, M. Boutonnet, S.G. Järas, Appl. Catal. B: Environ. 54 (2004) 193.
[40] K. Foger, D. Hay, H. Jaeger, J. Catal. 96 (1985) 154.
[41] P.O. Thevenin, A. Alcalde, L.J. Pettersson, S.G. Järas, J.L.G. Fierro, J. Catal. 215 (2003) 78.
[42] J.F. Moulder, W.F. Stickle, P.E. Sobol, K.D. Bomben, Handbook of X-ray Photoelectron Spectroscopy, Physical Electronics Inc., Minnesota, USA, 1995.
[43] S.Y. Christou, M.C. Álvarez-Galván, J.L.G. Fierro, A.M. Efstathiou, Appl. Catal. B: Environ. 106 (2011) 103.
[44] L. Kepiński, M. Wolcyrz, J. Solid State Chem. 131 (1997) 121.
[45] S. Bernal, J.J. Calvino, M.A. Cauqui, J.M. Gatica, C. Larese, J.A.P. Omil, J.M. Pintado, Catal. Today 50 (1999) 175.
[46] P. Fornasiero, R. Di Monte, G.R. Rao, J. Kašpar, S. Meriani, A. Trovarelli, M. Graziani, J. Catal. 151 (1995) 168.
[47] E. Rogemond, R. Fréty, V. Perrichon, M. Primet, S. Salasc, M. Chevrier, C. Gauthier, F. Mathis, J. Catal. 169 (1997) 120.
[48] P. Vidmar, P. Fornasiero, J. Kašpar, G. Gubitosa, M. Graziani, J. Catal. 171 (1997) 160.
[49] H. Lieske, J. Volter, J. Phys. Chem. 89 (1985) 1841.
[50] T.C. Chang, J.J. Chen, C.T. Yeh, J. Catal. 96 (1985) 51.
[51] R.A. Daley, S.Y. Christou, A.M. Efstathiou, J.A. Anderson, Appl. Catal. B: Environ. 60 (2005) 117.
[52] X. Liu, O. Korotkikh, R. Farrauto, Appl. Catal. A: Gen. 226 (2002) 293.
[53] R.D.S. Monteiro, L.C. Dieguez, M. Schmal, Catal. Today 65 (2001) 77.
[54] D. Gao, S. Wang, C. Zhang, Z. Yuan, S. Wang, Chin. J. Catal. 29 (2008) 1221.
[55] E. Mamontov, R. Brezny, M. Koranne, T. Egami, J. Phys. Chem. B 107 (2003) 13007.
[56] S. Matsunaga, K. Yokota, S. Hyodo, T. Suzuki, H. Sobukawa, SAE Technical Paper Series 982706, 1998.
[57] S.Y. Christou, A.M. Efstathiou, Top. Catal. 42–43 (2007) 351.
[58] A. Kubacka, A. Martinez-Arias, M. Fernadez-Garcia, M.A. Newton, Catal. Today 145 (2009) 288.
[59] A. Iglesias-Juez, A. Martinez-Arias, M.A. Newton, S.G. Fiddy, M. Fernadez-Garcia, Chem. Commun. (2005) 4092.
[60] G.J. Arteaga, J.A. Anderson, S.M. Becker, C.H. Rochester, J. Mol. Catal. A: Chem. 145 (1999) 183.
[61] J. Fan, X. Wu, X. Wu, Q. Liang, R. Ran, D. Weng, Appl. Catal. B: Environ. 81 (2008) 38.
[62] M. Fernández-García, A. Martínez-Arias, A. Iglesias-Juez, A.B. Hungrıa, J.A. Anderson, J.C. Conesa, J. Soria, Appl. Catal. A: Gen. 231 (2001) 39.
[63] A. Martínez-Arias, M. Fernández-García, A. Iglesias-Juez, A.B. Hungría, J.A. Anderson, J.C. Conesa, J. Soria, Appl. Catal. B: Environ. 38 (2002) 151.
[64] A. Martínez-Arias, M. Fernández-García, A.B. Hungría, A. Iglesias-Juez, K. Duncan, R. Smith, J.A. Anderson, J.C. Conesa, J. Soria, J. Catal. 204 (2001) 238.
[65] M. Skotak, Z. Karpinski, W. Juszczyk, J. Pielaszek, L. Kepinski, D.V. Kazachkin, V.I. Kovalchuk, J.L. d'Itri, J. Catal. 227 (2004) 11.
[66] K. Kili, F.L. Normand, J. Mol. Catal. A: Chem. 140 (1999) 267.
[67] A. Iglesias-Juez, A.B. Hungria, A. Martinez-Arias, J.A. Anderson, M. Fernandez-Garcia, Catal. Today 143 (2009) 195.
[68] U. Oran, D. Uner, Appl. Catal. B: Environ. 54 (2004) 183.
[69] N. Kumar, T.S. King, R.D. Vigil, Chem. Eng. Sci. 55 (2000) 4973.
[70] K. Almusaiteer, S.S.C. Chuang, J. Catal. 184 (1999) 189.
[71] M. Haneda, Y. Kintaichi, I. Nakamura, T. Fujitani, H. Hamada, J. Catal. 218 (2003) 405.
[72] W.A. Brown, D.A. King, J. Phys. Chem. B 104 (2000) 2578.
[73] S.Y. Christou, A.M. Efstathiou, Top. Catal. 42–43 (2007) 415.
[74] P.S. Lambrou, A.M. Efstathiou, J. Catal. 240 (2006) 182.
[75] J.P. Dacquin, C. Dujardin, P. Granger, Catal. Today 137 (2008) 390.
[76] R. Eisenberg, C.D. Meyer, Acc. Chem. Res. 8 (1975) 26.